Electrochimica Acta 228 (2017) 586–596

Contents lists available at ScienceDirect

Electrochimica Acta

journal homepage: www.elsevier.com/locate/electacta

Electrochemical Studies on Corncob Derived Activated Porous Carbon for Supercapacitors Application in Aqueous and Non-aqueous Electrolytes

M. Karnan[a], K. Subramani[a,b], P.K. Srividhya[c], M. Sathish[a,b,*]

[a] Functional Materials Division, CSIR-Central Electrochemical Research Institute, Karaikudi- 630 003, Tamilnadu, India
[b] Academy of Scientific and Innovative Research (AcSIR), CSIR-Central Electrochemical Research Institute, Karaikudi- 630 003, Tamilnadu, India
[c] Department of Mechanical Engineering, Periyar Maniammai University, Thanjavur, India

ARTICLE INFO

Article history:
Received 6 December 2016
Received in revised form 9 January 2017
Accepted 16 January 2017
Available online 17 January 2017

Keywords:
corncob
porous carbon
supercapacitors
ionic liquids
bio-derived
high energy density

ABSTRACT

Corncob carbon prepared by means of (KOH) chemical activation method at 600 °C for 1 h is shown as a promising electrode material for supercapacitors. The XRD analysis of the activated corncob carbon shows highly amorphous and disordered structure. The specific surface area and pore volume of the activated carbon are analysed using Brunauer-Emmett-Teller (BET) method. The calculated BET surface area of activated corncob carbon is ~800 $m^2 g^{-1}$ with micro and mesoporous in nature. The porous nature of the carbon is further confirmed using SEM and HR-TEM analysis. The electrochemical studies in aqueous electrolytes reveal that a high specific capacitance of 390 $F g^{-1}$ at 0.5 $A g^{-1}$ current density. The electrochemical performance of activated corncob electrodes is studied in three different ionic liquids, among them the $EMIMBF_4$ possess good capacitive behaviour and the wide potential window resulted a high energy density of 25 Wh kg^{-1} and power density of 174 W kg^{-1}. The supercapacitor device fabricated using the ionic liquid could power a red LED for more than 4 min after upon 10 s charging. The above investigation clearly indicates that the corncob derived carbon materials are promising for applications in supercapacitor.

1. Introduction

The projected global demands in the energy sectors, depletion of fossil fuels, and growing environmental concern, there is an urgent need for the substantial developments in the energy storage and conversion devices [1]. The most common energy storage devices are batteries, capacitors and supercapacitors [2–6]. Among them supercapacitors has attracted considerable interest in recent days due to its high power density and long cyclability over the other energy storage devices [7–10]. Based on the energy storage mechanism, supercapacitors are broadly classified into electrochemical double layer capacitors (EDLC) by ion adsorption or pseudocapacitors by fast surface redox reactions [11,12]. Generally, EDLCs based supercapacitors are commercialized owing to the low cost, exceptional cycle life and high power density [13–15]. However, the low energy density of the supercapacitors limits their wide applications in electric and hybrid electric vehicles. The energy density of the supercapacitors mainly depends on the nature of the electrode materials and the working voltage of the device [16]. The most commonly used electrode materials are carbon based materials, metal oxides and conducting polymers [17–20]. The specific capacitance of the carbon based materials are mainly based on the EDLCs and its depend on the surface area of the materials [21,22]. Preparation of high surface area carbon without sacrificing the required conductivity is a challenge issue [11]. Thus, the EDLCs have poor specific capacitance while the pseudocapacitors have high specific capacitance where the specific capacitance depends on the surface or fast redox reactions [23–25]. The cycle life of EDLCs is much higher than the pseudocapacitors. Whereas, the operating potential of the EDLCs is higher than the pseudocapacitors due to high electrochemical stability of the carbon based materials [23,24]. Attempts are in progress to increase the energy density of the supercapacitors by combining the EDLCs and pseudocapacitance in such a way that both the operating voltage and the specific capacitance could be increased significantly [23,25,26].

* Corresponding author at: Functional Materials Division, CSIR-Central Electrochemical Research Institute, Karaikudi- 630 003, Tamilnadu, India.
E-mail addresses: marappan.sathish@gmail.com, msathish@cecri.res.in (M. Sathish).

http://dx.doi.org/10.1016/j.electacta.2017.01.095
0013-4686/

On the other hand the working voltage of the supercapacitors could be increased by using non-aqueous electrolytes. Attempts have been made to use various organic electrolytes and ionic liquids, and the working voltage of the supercapacitors have been increased significantly [23,27,28]. However, the slow diffusion of ions, high viscosity of the organic electrolytes and poor electrode kinetics in organic electrolytes limits the energy density [29]. Thus, the design and synthesis of carbon materials with desired meso and micro porous nature is highly essential for supercapacitors application in organic electrolytes. Thus, various carbon materials including fullerene based nanostructured materials have been designed and prepared to address the various challenges [30,31]. Recently, bio-derived activated carbon materials have been investigated due to their higher surface area, good conductivity, abundance and low cost [32–34]. The bio-derived activated carbon materials are obtained from different sources such as firwood [35,36], banana fiber [37], nutshell [38], ricehusk [39], sunflower seed shell [40], cherry stone [41] and corn grain [42]. An overall literature-review for various bio-derived activated carbon based supercapacitors is listed in Table ST1. The chemical activation of bio-derived carbon resulted to formation of meso and micro porous carbon materials, and they have been shown promising application in supercapacitors due to the enhanced specific capacitance [43,44] and improved energy density [45,46]. The specific surface area and pore formation of the activated carbon mainly depends on activation temperature. Thus, the activation temperature for the bio-derived materials has been studied between 400–900 °C in the reported literature. In general, high temperature activation results the formation of conductive carbon due to the removal of all the functional groups, but it has various disadvantages like lower yield, pore-size shrinking, poor pseudocapacitance due to the absence of functional groups and poor surface area of the electrode materials. On the other hand, low temperature activation results carbon with poor conductivity and high pseudocapacitance without long term stability. Thus, the optimization of activation temperature is highly warranted to obtain high specific capacitance with long term stability. In the present study, the activation temperature was varied to 600, 700 and 800 °C for corncob derived carbon and based on the electrochemical performance it was optimised to 600 °C for the further characterization. Recently, Matthew Genovese *et.al.,* [47] reported bio-mass residue corncob using nitrogen pyrolysis and high temperature thermal flash exfoliation. They have shown the exfoliated bio-char corn cob results with 221 F g^{-1} specific capacitance. Thus, the preparation of bio-derived carbon materials from various biomaterials with and without chemical activation has gathered much attention. M.P. Adhikari *et.al.* [48], reported nanoporous activated carbon derived from corncob for enhanced sensing and application in electrochemical supercapacitors with an specific capacitance of 340 F g^{-1} at 5 mV/s scan rate. L. Ding *et.al.* [49], reported new route for the conversion of corncob into porous carbon by hydrolysis followed by activation, and it showed a specific capacitance of 236 F g^{-1} at 1.25 A/g current density. W.H. Qu et al. [50], reported to conversion of bio-waste corncob residue into value added porous carbon for supercapacitor electrodes with an high specific capacitance of 314 F g^{-1} at 5 mV/s scan rate. Here, we demonstrate a facile way for the preparation of porous carbon material from bio-char corncob for supercapacitors application in aqueous and non-aqueous electrolytes. The corn is one of the healthy food materials and its centre part is thrown out as bio-waste. These waste part of the corncob was collected, carbonized and activated using KOH [51] to obtain the corncob derived porous carbon. The resulted electrode materials possess a high specific capacitance both in aqueous and ionic liquids. The supercapacitor device fabricated using the corncob carbon could power red LED for 4 min upon 10 s charging at 0.5 A g^{-1} current density.

2. Experimental section

2.1. Synthesis of Activated Corncob

Corncob derived activated carbon was prepared via carbonization followed by activation of carbonized materials. The typical carbonization and activation process as follows. The raw corncob waste materials collected from urbane land was slash into small pieces and washed with DI water for several times and dried at 100 °C for 48 h. Then, the dried corncob was carbonized at 400 °C in a tubular furnace under inert atmosphere (Ar) for 4 h. The carbonized corncob was grained well and subjected to chemical activation process, where KOH pellets and corncob material are mixed in the weight ratio of 3:1. Then the mixture was heat treated at 600, 700 and 800 °C in a tubular furnace under Ar atmosphere at a heating rate of 5 °C min^{-1} for 1 h. After activation, the resulting carbon materials was washed thoroughly with DI water for several times until the pH of the filtrate becomes 7, followed by ethanol and dried at 60 °C for 3 h. The dried sample was grained to fine powder and stored for further characterization. The carbonised corncob before activation was denoted as CC-BA and the KOH activated corncob after activation at 600, 700 and 800 °C were denoted as CC-AA-600, CC-AA-700 and CC-AA-800 in the further discussions, respectively.

2.2. Materials characterization

The crystalline nature of the synthesised materials was analysed using powder X-ray diffraction (PXRD) measurements using BRUKER D8 ADVANCE X-ray Diffractometer with Cu $K_\alpha$radiation (α=1.5418 Å). The 2θ values of XRD measurement were in the range of 10−80° at 0.02° steps with a count time of 0.2 s. The surface morphology of the sample was examined by scanning electron microscopy using TESCAN (Supra 55VP) operating at an accelerating voltage of 30 kV. Fourier transform infrared (FT-IR) spectra were revealed in TENSOR 27 spectrometer (Bruker) using KBr pellet technique from 400 to 4000 cm^{-1}. Thermogravimetric analysis (TGA) of CC-BA and CC-AA-600 were carried out by TGA/DTA (SDT Q 600) in a temperature ranging from room temperature to 900 °C in an inert (Ar, 99.9% pure) atmosphere. CHNS analysis was measured to estimate the amount of carbon content and hetero atom present in the samples using elementar vario EL III. The surface area of the CC-AA-600 was calculated using Quantachrome NOVA 3200e surface area and pore size analyser. The particle size and dispersion of activated carbon was examined using higher resolution transmission electron microscopy (HR-TEM, Tecnai G^2 TF20) working at an accelerating voltage of 200 kV.

2.3. Electrochemical measurement

The electrochemical behaviour of CC-BA, CC-AA-600, CC-AA-700 and CC-AA-800 was studied by Cyclic Voltammetry (CV), galvanostatic charge-discharge (CD) and electrochemical impedance spectroscopy (EIS) analysis. The working electrode was fabricated by mixing the carbon derived from corncob, super-p-carbon black and polytetrafluoroethylene (PTFE) in the weight ratio of 80:15:5 respectively. The resulting electrode paste (~2 mg) was pressed on a stainless steel mesh current collector. The electrochemical behaviour of corncob based electrode materials was studied in both three electrode and two electrode configuration using BioLogic SP-300. For the three electrode measurements, the corncob working electrode materials, a slice of Pt foil act as a counter electrode with saturated calomel electrode (SCE) as a reference electrode respectively. The CV experiments carried out from the potential range of −0.4 to 0.8 V at various scan rates

ranging from 10 to 50 mV/s. The charge-discharge cycling test was carried out at different current density ranging from 0.5 to 10 A g^{-1}. From the CD analysis the specific capacitance of the electrodes are calculated using the following equation [52]

$$C_{sp} = \frac{i \times \Delta t}{\Delta v \times m} \quad (1)$$

Where $C_{sp}(Fg^{-1})$ is the specific capacitance of the material, i current density (A/g), Δt is the discharge time (s), m is the active mass and Δv potential window of the electrode materials. In order to study the potential application of these electrode materials in supercapacitor, the electrode materials are investigated in a two electrode configuration. The whole electrochemical studies were measured in both aqueous (1 M H_2SO_4) and non-aqueous electrolyte solution (ionic electrolyte) in the potential range of −0.4 to 0.8 V and 0 to 3 V at various scan rate ranging from 10 to 50 mV/s, respectively. For CD analysis, we have analysed comparison study at 0.1 A g^{-1} current density for all the three ionic liquids. In the case of ionic liquid electrolytes, the electrode paste was converted into thin sheet and cut into small coin-like working electrodes. Pt was used as current collector with whatmann filter paper as separator placed in between the anode and cathode materials. The specific capacitance, energy density and power density was calculated using the following equation [53]

$$C_t = \frac{I\Delta t}{m\Delta V} \quad (2)$$

$$C_{sp} = 4C_t \quad (3)$$

$$E = \frac{1}{2}C_t(\Delta V)^2 \quad (4)$$

$$P = \frac{E_t}{\Delta t} \quad (5)$$

Where, C_t (F g^{-1}) is the total specific capacitance, C_{sp} is the specific capacitance of the electrode materials (F g^{-1}), I is the current (A), Δt is the discharge time (sec), m is the total active mass of the electrodes (g), ΔV is the cell voltage (V), E (Wh kg^{-1}) is the energy density and P (W kg^{-1}) is the power density.

3. Results and discussion

The chemical activation processes for carbon based materials were generally made by mixing with activating agents like KOH, NaOH, $ZnCl_2$, and H_3PO_4. The activation process will give rise to porosity with high surface area. Compared to physical activation method, chemical activation is superior due to less activation time, single step process, high yield, and high specific surface area [54]. The preparation of corncob derived activated porous carbon is shown in Scheme 1.

The XRD pattern of CC-AA-600 shows (Fig. 1a) two broad peaks around 23 and 43° is corresponding to (002) and (100) planes, respectively. The CC-BA showed an additional peaks at 11° (shown as *) indicates more oxygen functional groups in the sample. The observed diffraction lines are significantly broader that indicates the more amorphous and disordered nature of CC-BA. Fig. 1b shows the FT-IR spectrum of CC-BA and CC-AA-600 from 400 to 4000 cm^{-1}. The O-H stretching observed around 3429 cm^{-1} was mainly attributed to chemisorbed water molecules and hydroxyl groups on the materials. And, the C-H the observed stretching around 2900 cm^{-1} and C=C stretching around 1629 cm^{-1} are assigned to the characteristic olefinic group it shows that the graphitisation is very much increased for CC-AA-600 sample. Compared to CC-BA the number of vibrational modes are largely diminished due to the reduction of functional groups in the CC-AA-600. The elements present in the mixture was analysed using CHNS

Scheme 1. Schematic representation of preparation of corncob derived activated porous carbon.

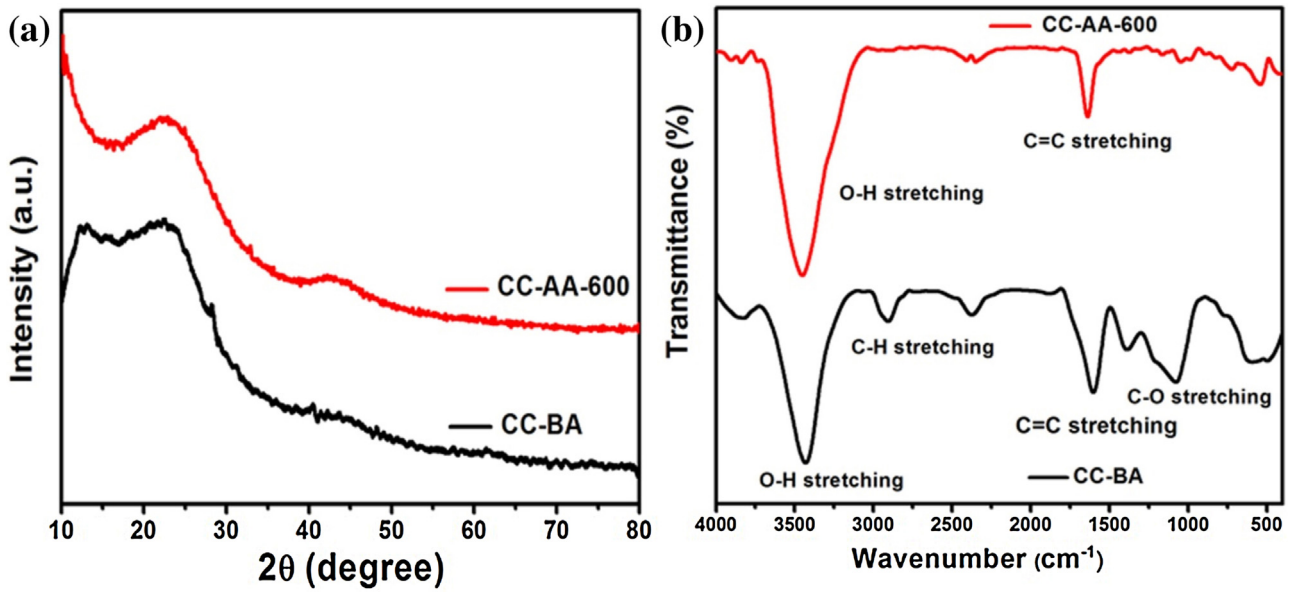

Fig. 1. XRD pattern (a) and FT-IR spectrum (b) of CC- BA and CC-AA-600.

analysis, the CC-AA-600 showed a carbon content of >70%. The elemental composition of CC-BA and CC-AA-600 samples were analysed using CHNS analysis, the results reveal that there is no substantial amount of hetero atoms such as sulphur and nitrogen content in the sample. CHNS data for all the samples are shown in Table ST2.

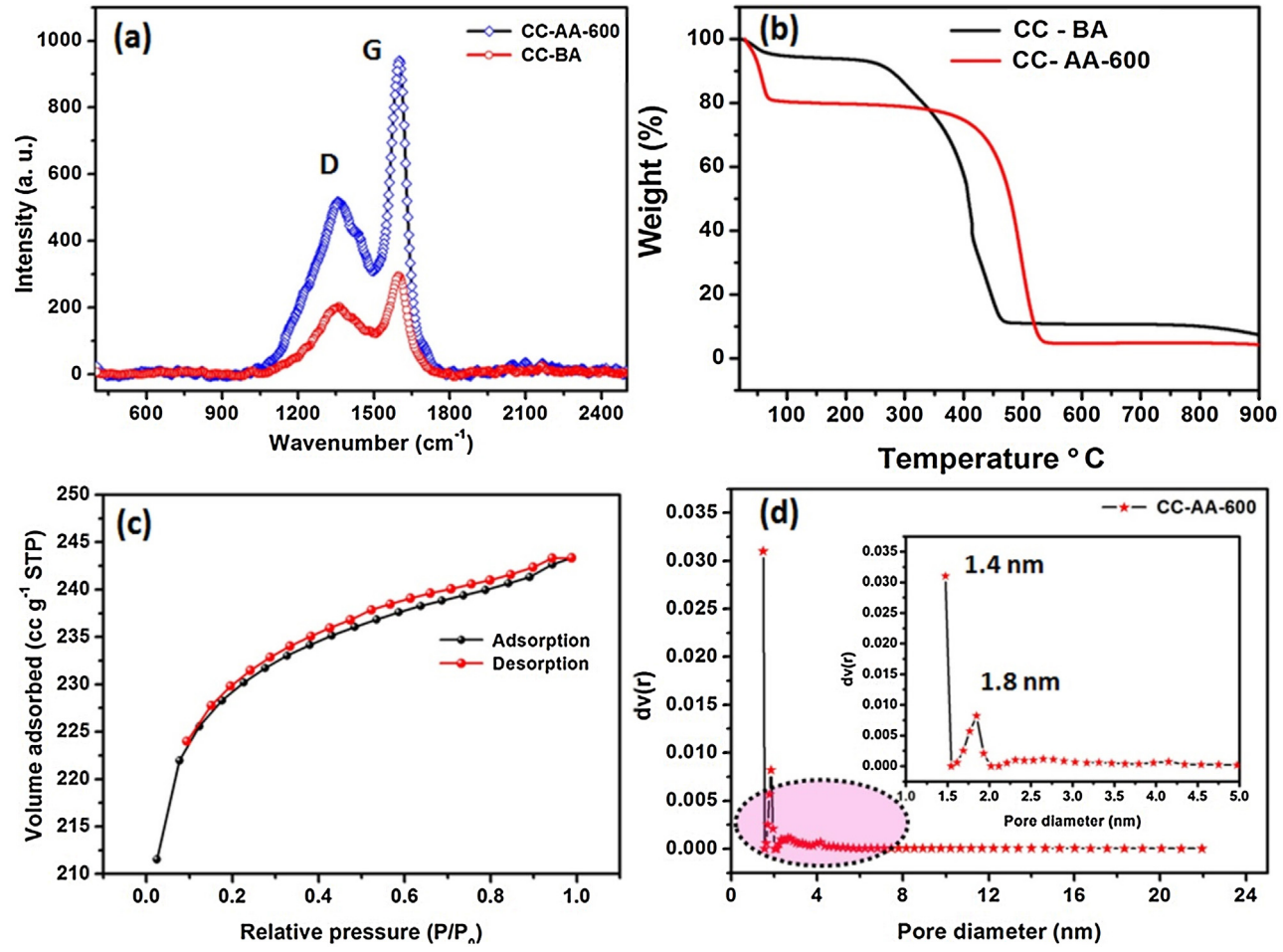

Fig. 2. (a) Raman spectroscopic analysis of CC-AA-600 and CC-BA, (b) TGA profile of CC-BA and CC-AA-600, (c) BET nitrogen adsorption-desorption isotherm of CC-AA-600 sample (d) its corresponding pore size distribution curve fitting using the DFT model.

Raman spectroscopy is a potential analytical tool to evaluate the degree of functionalization before and after carbonization/activation in the bio-derived carbon materials (Fig. 2a). Usually, the intensity ratio (I_D/I_G) of D band (I_D) and G band (I_G) reveals the degree of defective nature and the extend of graphitization. Both the CC-BA and CC-AA-600 samples show a characteristic D and G

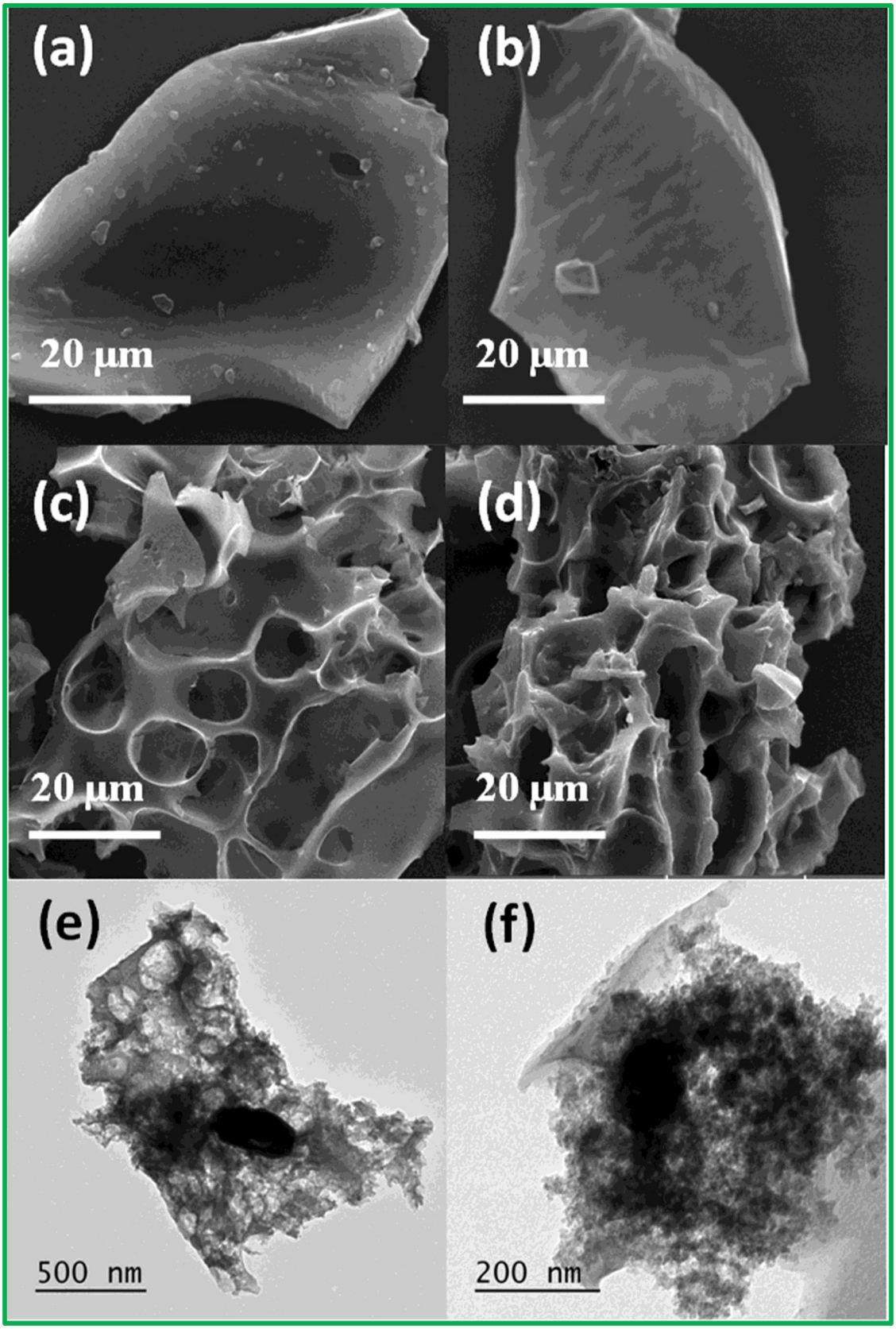

Fig. 3. SEM images of (a-b) CC-BA, (c-d) CC-AA-600 and (e-f) HR-TEM images of CC-AA-600.

bands at 1363 and 1603 cm^{-1}, respectively. The calculated I_D/I_G ratio value 0.76 and 0.57 for CC-BA and CC-AA-600, respectively indicates that the high temperature activation process increased the degree of graphitization by removal of surface functional group and defect structure, which is in good agreement with the FT-IR observations. The TGA profile of CC-BA shows a minimum weight loss below 100 °C due to adsorbed moisture, and then a major weight loss was observed between 280 to 480 °C due to the decomposition of carbon molecules (Fig. 2b). Whereas in CC-AA-600, the large 20 wt.% weight loss was observed below 100 °C

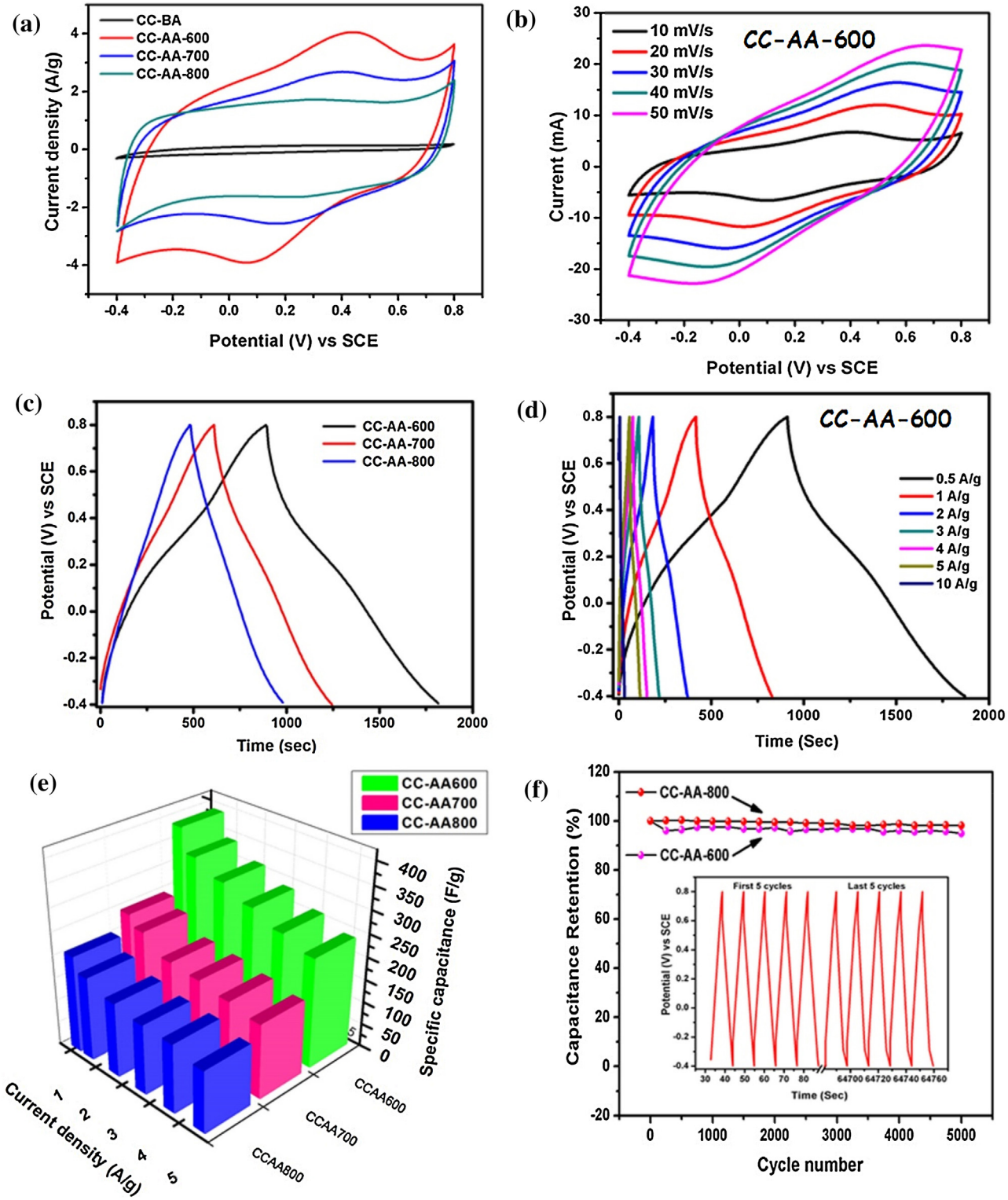

Fig. 4. (a) CV profile of all corncob derived materials at scan rate of 10 mV/s (b) CV profile of CC-AA-600 electrode at different scan rates, (c) CD profile of corncob derived materials at a current density of 0.5 A/g (d) CD profile of CC-AA-600 electrode at different current densities (e) Specific capacitance of corncob derived carbon electrodes as a function of current densities (f) Cyclability profile of CC-AA-600 and CC-AA-800 electrodes at 10 A/g in three electrode cell, and the first and last 5 charge-discharge cycles of CC-AA-600 (inset).

indicating the large amount of moisture than the CC-BA. After 100 °C there is a stable thermogravimetric profile was observed up to 400 °C, then a sharp weight loss was observed due to the decomposition of carbon. The TGA profile of CC-AA-600 is neat and clean when compared to CC-BA, indicating that the KOH activation results the formation of structurally stable carbon atoms (Fig. 2b). The surface area and porosity of the CC-AA-600 was studied using the BET nitrogen adsorption-desorption isotherm (Fig. 2c). The CC-AA-600 materials show a high specific surface area of 800 $m^2 g^{-1}$. The pore size distribution curve based on the DFT model indicates the presence of micro and mesopores in the range of 1.4 – 1.8 and 2.2 – 5 nm with an average pore volume of 0.337 $cm^3 g^{-1}$, respectively (Fig. 2d).

The SEM images of CC-BA (Fig. 3a & b) showed the formation of micron size particles without any pores over the surface, whereas the SEM image of CC-AA-600 (Fig. 3c & d) clearly confirms the formation of micro-size pores throughout out the sample. The above observation clearly confirmed that KOH activation of carbon results the formation of pores over the carbon materials. Though, the nanometre size pores are not seen in SEM images and it was evidently confirmed using HR-TEM analysis. The HR-TEM images of CC-AA-600 clearly showed the micro and mesopores over the surface (Fig. 3e & f).

The electrochemical behaviour of activated corncob was investigated in both aqueous and non-aqueous electrolytes. In the case of aqueous electrolytes, 1 M H_2SO_4 is used and the electrochemical studies were carried out in both three and two electrodes configuration. In a three electrode cells, the activated corncob material, SCE and the platinum mesh were used as working, reference and counter electrodes respectively. The CV and CD profiles were recorded at different scan rates and current densities, respectively. Fig. 4a shows the CV profile of CC-BA, CC-AA-600, CC-AA-700 and CC-AA-800 samples in the potential window of −0.4 to 0.8 V *Vs* SCE. It can be clearly seen that the CC-AA-600 shows EDLC like behaviour with significant pseudocapacitive nature and the observed current is significantly higher than the counterpart before the activation (CC-BA). When the activation temperature was increased to 700 and 800 °C, the specific capacitance was decreased compared to CC-AA-600 and the pseudocapacitive nature was also found to be decreased in CC-AA-700 and CC-AA-800 due to absence of functional groups, respectively. The presence of pseudocapacitive nature along with EDLC in CC-AA-600 could be clearly seen from the CV profiles carried at different scan rate (Fig. 4b). The CV profile at low scan rate clearly showed the quasi rectangular shape profile due to the presence of oxygen containing functional groups in the activated

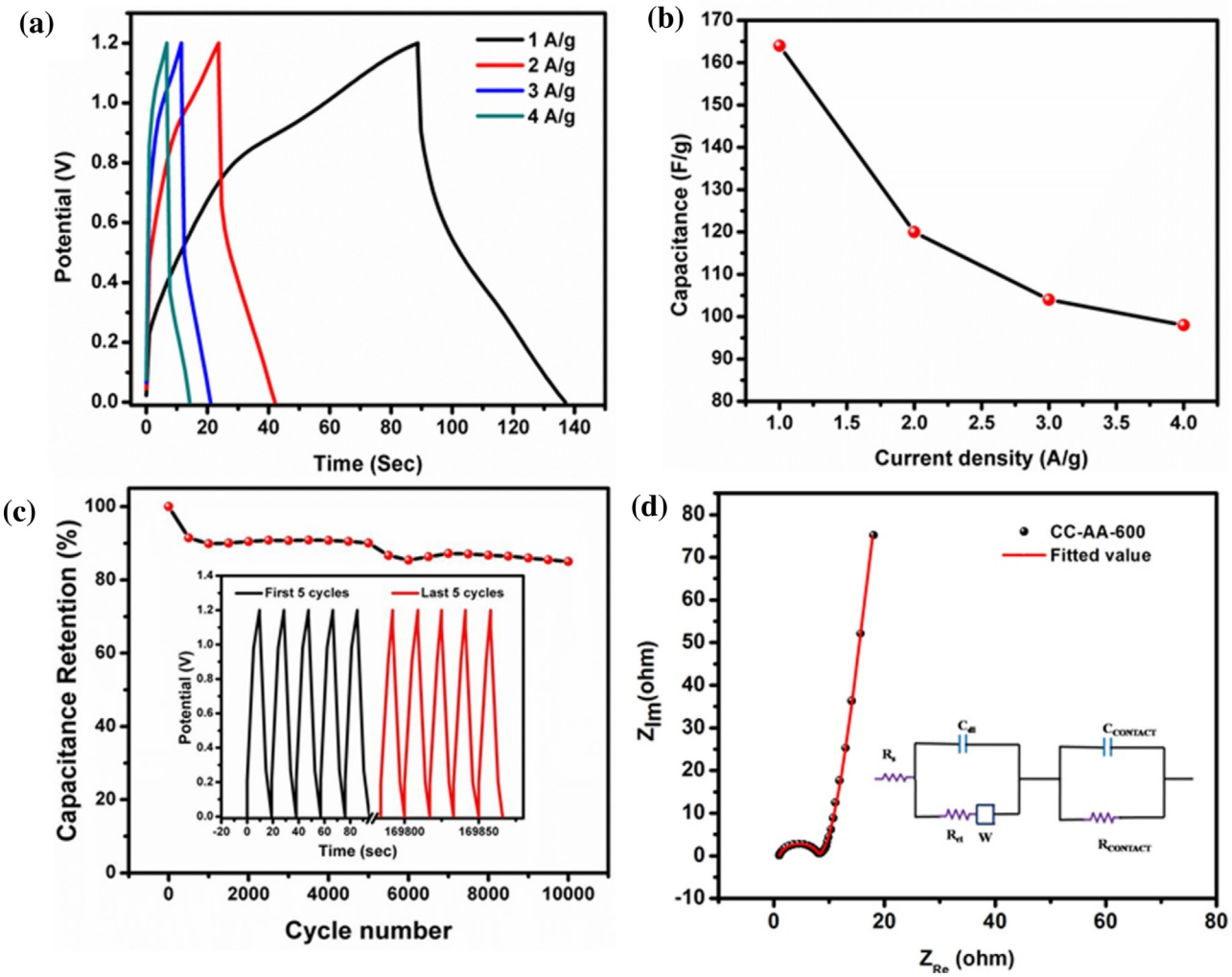

Fig. 5. (a) CD profile of CC-AA-600 electrodes in symmetric two electrode cell, (b) specific capacitance of CC-AA-600 electrodes in symmetric two electrode cell at different current density, (c) Cyclability of CC-AA-600 electrodes in symmetric two electrode cell at 4 A/g current density and (d) EIS spectrum of CC-AA-600 electrodes in symmetric two electrode cell and the corresponding equivalent circuit model (inset).

sample. The nonlinear discharge profile observed for the CC-AA-600, CC-AA-700 and CC-AA-800 confirmed that the presence of pseudocapacitive behaviour (Fig. 4c & Fig. S1). When the activation temperature increased the non-linear like trend was decreased significantly due to absence of the pseudocapacitance, it is in good agreement with the above CV studies. The specific capacitance of the CC-AA-600 electrode was calculated using the CD profile and a maximum specific capacitance of 390 F g^{-1} was obtained at 0.5 A g^{-1} current density (Fig. 4d). When the current density was increased from 1, 2, 3, 4 and 5 A g^{-1} the specific capacitance was decreased gradually from 338, 311, 285, 260 and 238 F g^{-1}, respectively. For comparison, the specific capacitance values at all the current densities are tabulated in Table ST3. The specific capacitance of CC-AA-600, CC-AA-700 and CC-AA-800 electrode at 0. 5A/g current density clearly showed the effect of activation temperature (Fig. S2). The rate performance of CC-AA-600, CC-AA-700 and CC-AA-800 electrode showed almost similar capacitance retention of 61, 64 and 64% when the current density was increased from 0.5 to 5 A/g, respectively (Fig. 4e). Generally, at low charging rate the diffusion of electrolyte through the micro and meso porous surfaces will enhance the electrochemical activity there by the specific capacitance will be improved significantly. However, at high charging rates the electrolyte can access only limited meso porous which will reduce the specific capacitance significantly. Though, the high temperature activation process increases the rate performance, its not very significant compared to CC-AA-600 sample. Similarly, the long term stability of CC-AA-600 and CC-AA-800 electrodes was studied for 5000 cycles of charge-discharge at 10 A g^{-1} (Fig. 4f). The CC-AA-600 electrode showed a 94% of intital specific capacitance while the CC-AA-800 electrode showed 98% of initial capacitacne after 5000 cycles of charge-discharge. Though, the CC-AA-800 will be the better candidate for supercapacitor device based applications the stability of the electrode compared to CC-AA-600 is not much improved due to the high temperature activation. Therefore, the activation temperature for the corncob derived activated porous carbon was optimised and fixed at 600 °C for further investigations.

To evaluate the potential application of CC-AA-600 in electrochemical supercapacitors experiments were carried out using two electrode symmetric configuration. Fig. 5a shows the CD profile of CC-AA-600 electodes in symmertic cell at a potential range of 0 to 1.2 V in 1 M H_2SO_4 electrolyte. A maximum specific capacitance of 164 F g^{-1} was obtained at 1 A g^{-1} and when the current density is increased from 2, 3 and 4 A g^{-1} the calcualted capacitance are 120, 104 and 98 F g^{-1}, respectively (Fig. 5b). To study the stability of the electrodes in the two electrode system, charge-discharge cycling

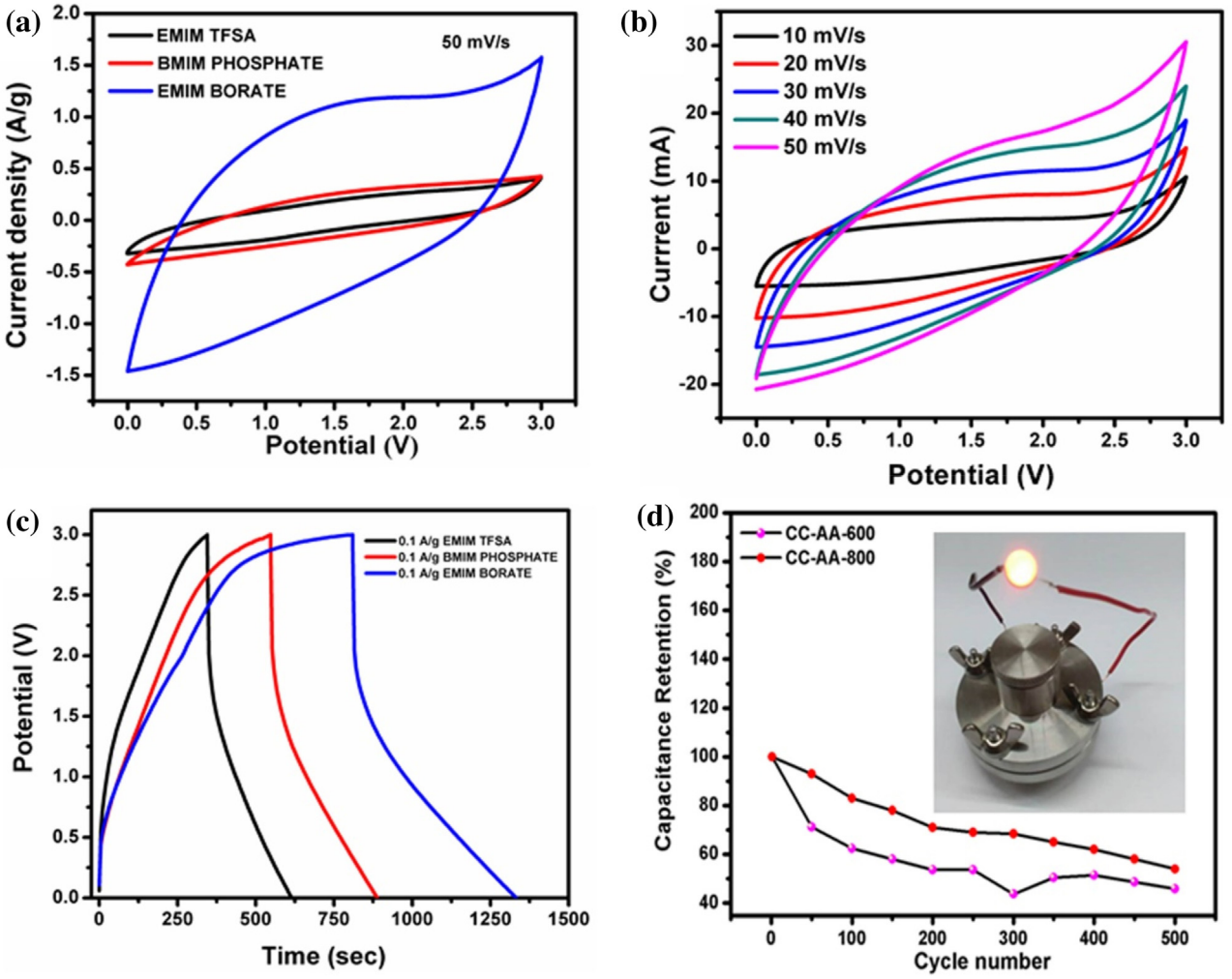

Fig. 6. (a) CV profile of CC-AA-600 symmetric two electrode cell in three different ionic liquids (b) CV profile of CC-AA-600 symmetric two electrode cell in EMIM borate (c) CD profile of CC-AA-600 symmetric two electrode cell at 0.1 A/g current rate in three different ionic liquids, (d) cyclability profile of CC-AA-600 and CC-AA-800 symmetric two electrode cell for 500 cycles at 0.1 A/g current density in EMIM borate and the photograph of CC-AA-600 symmetric two electrode cell in EMIM borate powered red LED (Inset).

was carried out for 10000 cycles at 4 A g^{-1}current density (Fig. 5c). A 85% of intital capacitance retention was observed at the end of 10000 cycles of charge-discharge. Inorder to understand the various resistance such as internal resistance, charge-transfer ressitance and solution resistance, electrochemical impedance spectroscopic (EIS) analysis were carried out at the frequency range of 100 kHz to 10 mHz with a amplitude of 10 mV (Fig. 5d). The obtained EIS was fitted with a appropriate equivalent circuit model (Fig. 5d inset) with the physical components such indicates the solution resistance (R_s), chargetransfer resistance (R_{ct}) and double layer capacitance (C_{dl}), respectively. The numerical values derived from the fitted profile reveals that the $R_s$value is very low in the range of 0.9 Ω and also it possessvery low charge transfer resistance of 8.4 Ω. And the vertical slope appears in the low-frequency region represents a ideal capacitive behaviour of CC-AA-600 electrode material.

To increase the energy density of the supercapacitors whether the specific capacitance or the working potential window has to be increased as much as possible. The later has more significance than the former according to the equation (4). However, the most commonly used aqueous electrolytes have its own limitation that the working voltage cannot be increase beyond the water decomposition potential. Recently, it was shown that the ionic liquids are stable up to 5 V and has lot of potential in energy storage devices as electrolyte [55–58]. Thus, the CC-AA-600 electrode has been studied with three different ionic liquids namely1-ethyl-3-methyl imidazoliumbistrifluro methyl sulfonyl amide [EMIM] [TFSA], 1-n-butyl-3-methyl imidazoliumhexafluro phosphate [BMIM] [PF_6] and 1-ethyl-3-methyl imidazolium tetra fluro borate [EMIM][BF_4]. Fig. 6a shows the CV profile of CC-AA-600 symmetric cell in the three ionic liquids at 50 mV/s scan rate. The CV profile clearly indicates that the all the three electrolytes and the CC-AA-600 electrode are stable for 3 V. And, the CC-AA-600 electrode showed better performance in EMIM borate electrolytes than the other two electrolytes.

Fig. 6b shows CV profile of CC-AA-600 electrode in EMIM borate electrolytes at different scan rates. The CV profile clearly indicates that the CC-AA-600 electrode in EMIM borate electrolytes is stable at all the scan rates and the capacitance mainly arises from EDLC than the pseudocapacitance. This may be ascribed to the absence of redox reaction that usually takes place in aqueous electrolytes. Also, the observed high specific capacitance may be due to the high conductivity of EMIM borate electrolyte compared to other two ionic liquids [59,60]. Fig. 6c shows the CD profile of CC-AA-600 electrode in all the three ionic liquid electrolytes at a constant current density of 0.1 A g^{-1}. The CD profiles clearly confirm that the specific capacitance of CC-AA-600 electrode is high in EMIM borate electrolyte, this is in good agreement with the CV studies. The CC-AA-600 electrode shows a specific capacitance of 80, 45 and 35 F g^{-1} in EMIM borate, BMIM phosphate and EMIM-TFSA electrolytes, respectively.

The calculated energy density of the CC-AA-600 symmetric cell is 25 Wh kg^{-1}, which is significantly higher than the supercapacitors in aqueous electrolyte. The cycling performance of CC-AA-600 and CC-AA-800 electrodes was evaluated for 500 cycle at 0.1 A g^{-1} current density (Fig. 6d). It can be clearly seen that in CC-AA-600 electrode a 50% of initial specific capacitance was retained after 500 cycles of charge-discharge while the CC-AA-800 electrode shows 54% of initial capacitacne. This is in good aggrement with our earlier observation that the high temperature activation at 800 °C does not help much to increase the stability of the electrode. The poor specific capacitance retention in ionic liquid medium is attributed to the large decrease in the structural stability of the electrode due to volume change during charge-discharge. Fig. 6d inset shows the symmetric supercapacitor device fabricated using CC-AA-600 electrodes, the charging time required for this device is less than 10 s at a low current rate of 0.5 A g^{-1} and it could power red LED for more than 4 min. The above experiments in aqueous and non-aqueous ionic liquid medium clearly confirms that the CC-AA-600 electrodes are promising material for electrochemical supercapacitor applications. The porous carbon materials derived from the waste corncob through economic route and the simple chemical activation process makes this material for viable application in electrochemical supercapacitors.

4. Conclusions

The corncob derived activated carbon based electrodes have been studied extensively for their application in supercapacitors both in aqueous and ionic liquids electrolytes. The chemical activation of corncob derived carbon materials with KOH results the formation of amorphous carbon with meso and micro porous in nature. The amorphous nature of the carbon was confirmed using XRD and the BET analysis revealed the porous nature. The formation of micro and meso porous on the corncob carbon was further confirmed using SEM and HR-TEM analysis. The corncob derived activated carbon showed maximum specific capacitance of 390 F g^{-1} at 0.5 A g^{-1}current density in aqueous three electrode cell. In a two electrode aqueous system it showed a maximum specific capacitance of 164 F g^{-1} at 1 A g^{-1}. The symmetric supercapacitor device fabricated using activated corncob carbon electrodes could power red LED for more than 4 min upon charging for 10 s at 0.5 A g^{-1} current density. This clearly shows that the corncob bio-waste derived activated carbon materials are good for supercapacitors applications. The low cost, abundant and environment friendly derived bio-carbon based electrode materials are viable for electrochemical energy storage applications.

Acknowledgements

The authors thank the Science & Engineering Research Board, Department of Science and Technology (GAP 07/14, DST-SERB), India for financial support. Mr K. Subramani (IF131153) thanks DST for INSPIRE Fellowship. The authors thank the Central Instrumentation Facility, CECRI, Karaikudi.

Appendix A. Supplementary data

Supplementary data associated with this article can be found, in the online version, at http://dx.doi.org/10.1016/j.electacta.2017.01.095.

References

[1] D. Liu, C. Fu, N. Zhang, H. Zhou, Y. Kuang, Three-Dimensional Porous Nitrogen doped Graphene Hydrogel for High Energy Density supercapacitors, Electrochim. Acta 213 (2016) 291–297, doi:http://dx.doi.org/10.1016/j.electacta.2016.07.131.
[2] D.U. Eberle, D.R. von Helmolt, Sustainable transportation based on electric vehicle concepts: a brief overview, Energy Environ. Sci. 3 (2010) 689, doi:http://dx.doi.org/10.1039/c001674h.
[3] N.A. Kumar, H.J. Choi, Y.R. Shin, D.W. Chang, L. Dai, J.B. Baek, Polyaniline-grafted reduced graphene oxide for efficient electrochemical supercapacitors, ACS Nano 6 (2012) 1715–1723, doi:http://dx.doi.org/10.1021/nn204688c.
[4] T.K. Shruthi, N. Ilayaraja, D. Jeyakumar, M. Sathish, Functionalization of graphene with nitrogen using ethylenediaminetetraacetic acid and their electrochemical energy storage properties, RSC Adv 4 (2014) 24248, doi:http://dx.doi.org/10.1039/c4ra02756f.
[5] P. Ning, X. Duan, X. Ju, X. Lin, X. Tong, X. Pan, et al., Facile synthesis of carbon nanofibers/MnO_2 nanosheets as high-performance electrodes for asymmetric supercapacitors, Electrochim. Acta 210 (2016) 754–761, doi:http://dx.doi.org/10.1016/j.electacta.2016.05.214.
[6] S.S. Balaji, A. Elavarasan, M. Sathish, High performance supercapacitor using N-doped graphene prepared via supercritical fluid processing with an oxime nitrogen source, Electrochim. Acta 200 (2016) 37–45, doi:http://dx.doi.org/10.1016/j.electacta.2016.03.150.

[7] S. Vijayakumar, S. Nagamuthu, G. Muralidharan, Porous NiO/C nanocomposites as electrode material for electrochemical supercapacitors, ACS Sustain. Chem. Eng. 1 (2013) 1110–1118, doi:http://dx.doi.org/10.1021/sc400152r.

[8] C. Portet, P.L. Taberna, P. Simon, E. Flahaut, C. Laberty-Robert, High power density electrodes for Carbon supercapacitor applications, Electrochim. Acta 50 (2005) 4174–4181, doi:http://dx.doi.org/10.1016/j.electacta.2005.01.038.

[9] L.L. Zhang, X.S. Zhao, Carbon-based materials as supercapacitor electrodes, Chem. Soc. Rev. 38 (2009) 2520–2531, doi:http://dx.doi.org/10.1039/b813846j.

[10] B.E. Conway, Electrochemical Supercapacitors scientific fundamental and technological applications (1999).

[11] P. Simon, Y. Gogotsi, Materials for electrochemical capacitors, Nat. Mater. 7 (2008) 845–854, doi:http://dx.doi.org/10.1038/nmat2297.

[12] K. Wang, Y. Cao, X. Wang, Q. Fan, W. Gibbons, T. Johnson, et al., Pyrolytic cyanobacteria derived activated carbon as high performance electrode in symmetric supercapacitor, Energy 94 (2016) 666–671, doi:http://dx.doi.org/10.1016/j.energy.2015.10.047.

[13] D.-D. Zhou, W.-Y. Li, X.-L. Dong, Y.-G. Wang, C.-X. Wang, Y.-Y. Xia, A nitrogen-doped ordered mesoporous carbon nanofiber array for supercapacitors, J. Mater. Chem. A. 1 (2013) 8488, doi:http://dx.doi.org/10.1039/c3ta11667k.

[14] M. Sevilla, R. Mokaya, Energy storage applications of activated carbons: supercapacitors and hydrogen storage, Energy Environ. Sci. 7 (2014) 1250–1280, doi:http://dx.doi.org/10.1039/C3EE43525C.

[15] M. Zhi, F. Yang, F. Meng, M. Li, A. Manivannan, N. Wu, Effects of pore structure on performance of an activated-carbon supercapacitor electrode recycled from scrap waste tires, ACS Sustain. Chem. Eng. 2 (2014) 1592–1598, doi:http://dx.doi.org/10.1021/sc500336h.

[16] B. Amutha, M. Sathish, A 2 V asymmetric supercapacitor based on reduced graphene oxide-carbon nanofiber-manganese carbonate nanocomposite and reduced graphene oxide in aqueous solution, J. Solid State Electrochem. 19 (2015) 2311–2320, doi:http://dx.doi.org/10.1007/s10008-015-2867-y.

[17] M. Sathish, S. Mitani, T. Tomai, I. Honma, MnO_2 assisted oxidative polymerization of aniline on graphene sheets: Superior nanocomposite electrodes for electrochemical supercapacitors, J. Mater. Chem. 21 (2011) 16216, doi:http://dx.doi.org/10.1039/c1jm12946e.

[18] K. Subramani, D. Jeyakumar, M. Sathish, Manganese hexacyanoferrate derived Mn_3O_4 nanocubes-reduced graphene oxide nanocomposites and their charge storage characteristics in supercapacitors, Phys. Chem. Chem. Phys. 16 (2014) 4952–4961, doi:http://dx.doi.org/10.1039/c3cp54788d.

[19] K. Wang, Y. Cao, X. Wang, P.R. Kharel, W. Gibbons, B. Luo, et al., Nickel catalytic graphitized porous carbon as electrode material for high performance supercapacitors, Energy 101 (2016) 9–15, doi:http://dx.doi.org/10.1016/j.energy.2016.01.059.

[20] V. Kuzmenko, O. Naboka, M. Haque, H. Staaf, G. Goransson, P. Gatenholm, et al., Sustainable carbon nanofibers/nanotubes composites from cellulose as electrodes for supercapacitors, Energy 90 (2015) 1490–1496, doi:http://dx.doi.org/10.1016/j.energy.2015.06.102.

[21] E. Frackowiak, Carbon materials for supercapacitor application, Phys. Chem. Chem. Phys. 9 (2007) 1774–1785, doi:http://dx.doi.org/10.1039/b618139m.

[22] L. Borchardt, M. Oschatz, S. Kaskel, Tailoring porosity in carbon materials for supercapacitor applications, Mater. Horizons 1 (2014) 157–168, doi:http://dx.doi.org/10.1039/C3MH00112A.

[23] G.P. Wang, L. Zhang, J.J. Zhang, A review of electrode materials for electrochemical supercapacitors, Chem. Soc. Rev. 41 (2012) 797–828, doi:http://dx.doi.org/10.1039/C1cs15060j.

[24] Y. Zhang, H. Feng, X. Wu, L. Wang, A. Zhang, T. Xia, et al., Progress of electrochemical capacitor electrode materials: A review, Int. J. Hydrogen Energy 34 (2009) 4889–4899, doi:http://dx.doi.org/10.1016/j.ijhydene.2009.04.005.

[25] B.E. Conway, V. Birss, J. Wojtowicz, The role and utilization of pseudocapacitance for energy storage by supercapacitors, J. Power Sources 66 (1997) 1–14, doi:http://dx.doi.org/10.1016/S0378-7753(96)02474-3.

[26] S.S. Balaji, M. Sathish, Supercritical fluid processing of nitric acid treated nitrogen doped graphene with enhanced electrochemical supercapacitance, RSC Adv. 4 (2014) 52256–52262, doi:http://dx.doi.org/10.1039/C4RA07820A.

[27] G.A. Snook, P. Kao, A.S. Best, Conducting-polymer-based supercapacitor devices and electrodes, J. Power Sources. 196 (2011) 1–12, doi:http://dx.doi.org/10.1016/j.jpowsour.2010.06.084.

[28] M. Sathish, S. Mitani, T. Tomai, I. Honma, Supercritical fluid assisted synthesis of N-doped graphene nanosheets and their capacitance behavior in ionic liquid and aqueous electrolytes, J. Mater. Chem. A 2 (2014) 4731–4738, doi:http://dx.doi.org/10.1039/C3ta15136k.

[29] H. Ohno, K. Fukumoto, Progress in Ionic Liquids for Electrochemical Reaction Matrices, Electrochemistry 76 (2008) 16–23, doi:http://dx.doi.org/10.5796/electrochemistry.76.16.

[30] P. Bairi, K. Minami, W. Nakanishi, J.P. Hill, K. Ariga, L.K. Shrestha, Hierarchically Structured Fullerene C_{70} Cube for Sensing Volatile Aromatic Solvent Vapors, ACS Nano 10 (2016) 6631–6637, doi:http://dx.doi.org/10.1021/acsnano.6b01544.

[31] L.K. Shrestha, R.G. Shrestha, Y. Yamauchi, J.P. Hill, T. Nishimura, K. Miyazawa, et al., Nanoporous carbon tubes from fullerene crystals as the π-electron carbon source, Angew. Chemie Int. Ed. 54 (2015) 951–955, doi:http://dx.doi.org/10.1002/anie.201408856.

[32] H. Jin, X. Wang, Z. Gu, J. Polin, Carbon materials from high ash biochar for supercapacitor and improvement of capacitance with HNO_3 surface oxidation, J. Power Sources 236 (2013) 285–292, doi:http://dx.doi.org/10.1016/j.jpowsour.2013.02.088.

[33] H. Sun, W. He, C. Zong, L. Lu, Template-free synthesis of renewable macroporous carbon via yeast cells for high-performance supercapacitor electrode materials, ACS Appl. Mater. Interfaces 5 (2013) 2261–2268, doi:http://dx.doi.org/10.1021/am400206r.

[34] X. He, P. Ling, J. Qiu, M. Yu, X. Zhang, C. Yu, et al., Efficient preparation of biomass-based mesoporous carbons for supercapacitors with both high energy density and high power density, J. Power Sources 240 (2013) 109–113, doi:http://dx.doi.org/10.1016/j.jpowsour.2013.03.174.

[35] F.-C. Wu, R.-L. Tseng, C.-C. Hu, C.-C. Wang, Physical and electrochemical characterization of activated carbons prepared from firwoods for supercapacitors, J. Power Sources 138 (2004) 351–359, doi:http://dx.doi.org/10.1016/j.jpowsour.2004.06.023.

[36] F.-C. Wu, R.-L. Tseng, C.-C. Hu, C.-C. Wang, Effects of pore structure and electrolyte on the capacitive characteristics of steam- and KOH-activated carbons for supercapacitors, J. Power Sources 144 (2005) 302–309, doi:http://dx.doi.org/10.1016/j.jpowsour.2004.12.020.

[37] R. Madhu, V. Veeramani, S.-M. Chen, Heteroatom-enriched and renewable banana-stem-derived porous carbon for the electrochemical determination of nitrite in various water samples, Sci. Rep. 4 (2014) 1–8, doi:http://dx.doi.org/10.1038/srep04679.

[38] A. Ahmadpour, D.D. Do, The preparation of activated carbon from macadamia nutshell by chemical activation, Carbon N. Y. 35 (1997) 1723–1732, doi:http://dx.doi.org/10.1016/S0008-6223(97)00127-9.

[39] X. He, P. Ling, M. Yu, X. Wang, X. Zhang, M. Zheng, Rice husk-derived porous carbons with high capacitance by $ZnCl_2$ activation for supercapacitors, Electrochim. Acta 105 (2013) 635–641, doi:http://dx.doi.org/10.1016/j.electacta.2013.05.050.

[40] X. Li, W. Xing, S. Zhuo, J. Zhou, F. Li, S.Z. Qiao, et al., Preparation of capacitor's electrode from sunflower seed shell, Bioresour. Technol. 102 (2011) 1118–1123, doi:http://dx.doi.org/10.1016/j.biortech.2010.08.110.

[41] M. Olivares-Marín, J.A. Fernández, M.J. Lázaro, C. Fernández-Gonzalez, A. Macias-Garcia, V. Gómez-Serrano, et al., Cherry stones as precursor of activated carbons for supercapacitors, Mater. Chem. Phys. 114 (2009) 323–327, doi:http://dx.doi.org/10.1016/j.matchemphys.2008.09.010.

[42] M.S. Balathanigaimani, W.-G. Shim, M.-J. Lee, C. Kim, J.-W. Lee, H. Moon, Highly porous electrodes from novel corn grains-based activated carbons for electrical double layer capacitors, Electrochem. Commun. 10 (2008) 868–871, doi:http://dx.doi.org/10.1016/j.elecom.2008.04.003.

[43] D.-D. Zhou, Y.-J. Du, Y.-F. Song, Y.-G. Wang, C.-X. Wang, Y.-Y. Xia, Ordered hierarchical mesoporous/microporous carbon with optimized pore structure for supercapacitors, J. Mater. Chem. A 1 (2013) 1192, doi:http://dx.doi.org/10.1039/c2ta00533f.

[44] S. Thieme, J. Brückner, I. Bauer, M. Oschatz, L. Borchardt, H. Althues, et al., High capacity micro-mesoporous carbon-sulfur nanocomposite cathodes with enhanced cycling stability prepared by a solvent-free procedure, J. Mater. Chem. A 1 (2013) 9225, doi:http://dx.doi.org/10.1039/c3ta10641a.

[45] Z. Li, Z. Xu, X. Tan, H. Wang, C.M.B. Holt, T. Stephenson, et al., Mesoporous nitrogen-rich carbons derived from protein for ultra-high capacity battery anodes and supercapacitors, Energy Environ. Sci. 6 (2013) 871–878, doi:http://dx.doi.org/10.1039/c2ee23599d.

[46] Z. Li, Z. Xu, H. Wang, J. Ding, B. Zahiri, C.M.B. Holt, et al., Colossal pseudocapacitance in a high functionality–high surface area carbon anode doubles the energy of an asymmetric supercapacitor, Energy Environ. Sci. 7 (2014) 1708–1718, doi:http://dx.doi.org/10.1039/c3ee43979h.

[47] M. Genovese, J. Jiang, K. Lian, N. Holm, High capacitive performance of exfoliated biochar nanosheets from biomass waste corn cob, J. Mater. Chem. A. 3 (2015) 2903–2913, doi:http://dx.doi.org/10.1039/C4TA06110A.

[48] M.P. Adhikari, R. Adhikari, R.G. Shrestha, R. Rajendran, L. Adhikari, P. Bairi, et al., Nanoporous activated carbons derived from agro-waste corncob for enhanced electrochemical and sensing performance, Bull. Chem. Soc. Jpn. 88 (2015) 1108–1115, doi:http://dx.doi.org/10.1246/bcsj.20150092.

[49] L. Ding, B. Zou, H. Liu, Y. Li, Z. Wang, Y. Su, et al., A new route for conversion of corncob to porous carbon by hydrolysis and activation, Chem. Eng. J. 225 (2013) 300–305, doi:http://dx.doi.org/10.1016/j.cej.2013.03.090.

[50] W.H. Qu, Y.Y. Xu, A.H. Lu, X.Q. Zhang, W.C. Li, Converting biowaste corncob residue into high value added porous carbon for supercapacitor electrodes, Bioresour. Technol. 189 (2015) 285–291, doi:http://dx.doi.org/10.1016/j.biortech.2015.04.005.

[51] M.A. Lillo-Ródenas, J. Juan-Juan, D. Cazorla-Amorós, A. Linares-Solano, About reactions occurring during chemical activation with hydroxides, Carbon N. Y. 42 (2004) 1365–1369, doi:http://dx.doi.org/10.1016/j.carbon.2004.01.008.

[52] L. Vinet, A. Zhedanov, A missing family of classical orthogonal polynomials, Science 345 (80) (2010) 20, doi:http://dx.doi.org/10.1126/science.1247727.

[53] K. Subramani, S. Kowsik, M. Sathish, Facile and Scalable Ultra-fine Cobalt Oxide/Reduced Graphene Oxide Nanocomposites for High Energy Asymmetric Supercapacitors, ChemistrySelect 1 (2016) 3455–3467, doi:http://dx.doi.org/10.1002/slct.201600792.

[54] J. Wang, S. Kaskel, KOH activation of carbon-based materials for energy storage, J. Mater. Chem. 22 (2012) 23710–23725, doi:http://dx.doi.org/10.1039/c2jm34066f.

[55] Y. Zhang, C. Shi, J.F. Brennecke, E.J. Maginn, Refined Method for Predicting Electrochemical Windows of Ionic Liquids and Experimental Validation Studies, J. Phys. Chem. B 118 (2014) 6250–6255, doi:http://dx.doi.org/10.1021/jp5034257.

[56] S.P. Ong, O. Andreussi, Y. Wu, N. Marzari, G. Ceder, Electrochemical windows of room-temperature ionic liquids from molecular dynamics and density

functional theory calculations, Chem. Mater. 23 (2011) 2979–2986, doi:http://dx.doi.org/10.1021/cm200679y.
[57] M. Hayyan, F.S. Mjalli, M.A. Hashim, I.M. AlNashef, T.X. Mei, Investigating the electrochemical windows of ionic liquids, J. Ind. Eng. Chem. 19 (2013) 106–112, doi:http://dx.doi.org/10.1016/j.jiec.2012.07.011.
[58] P.A.Z. Suarez, V.M. Selbach, J.E.L. Dullius, S. Einloft, C.M.S. Piatnicki, D.S. Azambuja, et al., Enlarged electrochemical window in dialkyl-imidazolium cation based room-temperature air and water-stable molten salts, Electrochim. Acta 42 (1997) 2533–2535, doi:http://dx.doi.org/10.1016/S0013-4686(96)00444-6.
[59] T. Herzig, C. Schreiner, H. Bruglachner, S. Jordan, M. Schmidt, H.J. Gores, Temperature and Concentration Dependence of Conductivities of Some New Semichelatoborates in Acetonitrile and Comparison with Other Borates, J. Chem. Eng. Data 53 (2008) 434–438, doi:http://dx.doi.org/10.1021/je700525h.
[60] S. Zhang, N. Sun, X. He, X. Lu, X. Zhang, Physical properties of ionic liquids: Database and evaluation, J. Phys. Chem. Ref. Data 35 (2006) 1475–1517, doi:http://dx.doi.org/10.1063/1.2204959.